Phonon Renormalization Induced by Electric Field in Ferroelectric Poly(Vinylidene Fluoride–Trifluoroethylene) Nanofibers

Lan Dong,[1,‡] Qing Xi,[1,‡] Jun Zhou,[1,†] Xiangfan Xu,[1,*] and Baowen Li[2]

[1]*Center for Phononics and Thermal Energy Science, China-EU Joint Center for Nanophononics, School of Physics Science and Engineering, Tongji University, Shanghai 200092, China*

[2]*Paul M. Rady Department of Mechanical Engineering and Department of Physics, University of Colorado, Boulder, Colorado 80309-0427, USA*

We report phonon renormalization induced by an external electric field $\mathbf{E}$ in ferroelectric poly (vinylidene fluoride–trifluoroethylene) [P(VDF-TrFE)] nanofibers through measuring the $\mathbf{E}$-dependent thermal conductivity. Our experimental results are in excellent agreement with the theoretical ones derived from the lattice dynamics. The renormalization is attributed to the anharmonicity that modifies the phonon spectrum when the atoms are pulled away from their equilibrium positions by the electric field. Our finding provides an efficient way to manipulate the thermal conductivity by tuning external fields in ferroelectric materials.

I. INTRODUCTION

The conventional phonon theory, which considers the anharmonicity as a perturbation, explains very well the behavior of thermal conductivity in crystals at low temperature. However, when the material is subject to an intensive external electric or magnetic field, or stress, or high temperature, the atoms deviate far away from their original equilibrium positions and consequently induce a strong anharmonicity that significantly modifies the phonon spectrum, and the perturbation theory is no longer valid. For example, at high temperature, thermal conductivities of some crystals are not inversely proportional to temperature, which is mainly attributed to large thermal motion of atoms at high temperature [1,2].

To incorporate the effect of anharmonicity into the conventional phonon transport theory, people usually renormalize the vibrational modes [3,4]. These renormalized vibrational modes are called *phonon renormalization*, which is more obvious in materials containing "rattlers," as those "rattlers" have much larger displacements than other atoms [5]. Another example to illustrate phonon renormalization is exposure of the materials to a stress, since stress could directly change the lattice structure of crystals and thus alter the elastic constants [6,7], leading to a change in thermal conductivity. Indeed, tuning thermal conductivity via stress has been widely adopted due to its

general applicability to materials, ranging from nanostructures [8–11], insulating solids [12], silicon nanowires [13], and semiconductor nanofilms [14], to organic polymers [7,15]. However, manipulating the thermal conductivity by changing temperature and stress is not easy for practical applications. People turn to other options such as applying electric or magnetic fields [16,17]. Electric-field-induced thermal switching has been studied in inorganic ferroelectric materials such as $PbTiO_3$ [18], $PbZr_{0.3}Ti_{0.7}O_3$ [19], and $BiFeO_3$ [20,21]. The variation of thermal conductivities under an electric field is mainly attributed to the electric-field-induced change of phonon-phonon scattering and domain wall densities.

Compared with inorganic materials, the change in thermal conductivity of organic materials under an electric field is rarely studied. Since the molecule chains of polymers are flexible and bendable, their thermal conductivity could be more sensitive to external field and easier to observe [15]. In the case of ferroelectric polymers with large polarizability, the dipole motion driven by the electric field is very likely to induce phonon renormalization. Among ferroelectric polymers, poly(vinylidene fluoride) (PVDF) and its copolymers are good prototypes for their outstanding piezoelectric [22] and ferroelectric properties [23,24].

In this work, we report an experimental observation of a tunable phonon renormalization in poly(vinylidene fluoride–trifluoroethylene) [P(VDF-TrFE)] nanofibers by measuring the electric-field-dependent thermal conductivity. The samples are fabricated by the electrospinning method and the thermal conductivity is then measured by

---

*xuxiangfan@tongji.edu.cn

†zhoujunzhou@tongji.edu.cn

‡These authors contributed equally to this work.

the thermal bridge method. We find that the measured electric field dependence of thermal conductivity, due to phonon renormalization, matches well with the analytically derived formula that considers the piezoelectric effect and the anharmonicity corresponding to thermal expansion. This finding provides an alternative way to manipulate the thermal conductivity in ferroelectric materials.

II. THEORETICAL MODEL

Figure 1 illustrates the concept of phonon renormalization induced by an electric field. As an example, a one-dimensional (1D) diatomic chain with one positive charge and one negative charge in each unit cell is shown in Fig. 1(a). The lattice constant is a and the separation between two atoms in each unit cell is b. The Taylor expansion of the potential energy can be written as

$$
\begin{aligned}
\Phi = \Phi^{(0)} &+ \frac{1}{2} \sum_{iv,i'v'} \Phi^{(2)}_{iv,i'v'} (\mathbf{X}_{iv} - \mathbf{X}^0_{iv})(\mathbf{X}_{i'v'} - \mathbf{X}^0_{i'v'}) \\
&+ \frac{1}{6} \sum_{iv,i'v',i''v''} \Phi^{(3)}_{iv,i'v',i''v''} (\mathbf{X}_{iv} - \mathbf{X}^0_{iv}) \\
&\times (\mathbf{X}_{i'v'} - \mathbf{X}^0_{i'v'})(\mathbf{X}_{i''v''} - \mathbf{X}^0_{i''v''}) + \dots,
\end{aligned}
\tag{1}
$$

where $\mathbf{X}_{iv} = \mathbf{R}_i + \mathbf{R}_v$ denotes the coordinate of the atom (i, v) referring to the vth atom in ith unit cell, $\mathbf{R}_i$ is the

position vector of the ith unit cell, and $\mathbf{R}_v$ is the location of the vth atom with respect to $\mathbf{R}_i$. $\Phi^{(0)}$ is a constant, while $\Phi^{(n)}$ is the nth-order derivative of the potential energy evaluated in the equilibrium configuration of atoms $\mathbf{X}^0_{iv}$. The potential of the positive atom near its equilibrium position is denoted by the solid curve in the lower graph of Fig. 1(a), and the harmonic term is specified in by the dashed curve. The force constants are determined by the harmonic term. It is convenient to qualitatively describe the quasi-1D molecular chain of P(VDF-TrFE) with the 1D diatomic chain model by treating CH2 and CF2 clusters as positively charged and negatively charged, respectively, as shown in Fig. 1(c).

When an electric field is adiabatically applied to the 1D diatomic chain as shown in Fig. 1(b), atoms are pulled away from their original equilibrium positions to new ones, $\tilde{\mathbf{X}}^0_{iv}$. The positive charge and the negative charge in each unit cell move in opposite directions. Consequently, the lattice constant changes from a to a' and the separation between two atoms in each unit cell changes from b to b'. The renormalized potential energy with respect to the new equilibrium positions is

$$
\tilde{\Phi} = \tilde{\Phi}^{(0)} + \frac{1}{2} \sum_{iv,i'v'} \tilde{\Phi}^{(2)}_{iv,i'v'} (\mathbf{X}_{iv} - \tilde{\mathbf{X}}^0_{iv})(\mathbf{X}_{i'v'} - \tilde{\mathbf{X}}^0_{i'v'}) + \dots,
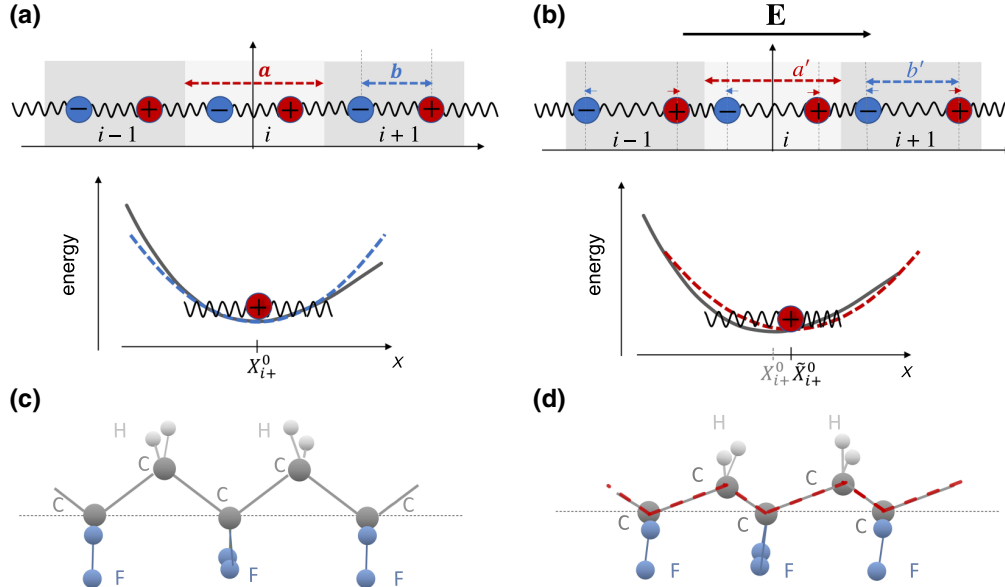\tag{2}
$$

FIG. 1. Schematic of the phonon renormalization in the case of an external electric field. (a) When there is no electric field, the diatomic chain is in equilibrium, with atoms locating at their equilibrium positions. The lattice constant is a and the separation between two atoms in each unit cell is b. The potential energy of atoms with positive charge is plotted by the black solid line, and a harmonic approximation is plotted by the blue dashed line. (b) After applying the external electric field, the atoms in the diatomic chain will be displaced from the original equilibrium positions. The lattice constant changes to a' and the separation between two atoms in each unit cell becomes b'. The harmonic approximation of the potential at the new equilibrium position will be different from the original one due to the anharmonicity. (c) Typical molecular chain structure of PVDF or similar polymers. (d) In the case of molecular chains, the variations of chain structure contain the change in bond angle and bond length.

where $\tilde{\Phi}^{(0)}$ is the reference energy in the presence of the electric field. It would be significantly changed by the change of equilibrium positions of atoms in comparison with $\Phi^{(0)}$. We believe that such a change does not affect the phonon renormalization because the relative distance between atoms is the key parameter rather than the reference energy. $\tilde{\Phi}^{(2)}_{iv,i'v'} = (\partial^2\tilde{\Phi}/\partial X_{iv}\partial X_{i'v'})|_0$ denotes the modified force constants. These can be calculated by comparing Eqs. (1) and (2), and the nearest neighboring terms are listed as follows:

$$\tilde{\Phi}^{(2)}_{i+,i+} = \Phi^{(2)}_{i+,i+} + \frac{1}{2}\left[\Phi^{(3)}_{i+,i+,i+} - \Phi^{(3)}_{i+,i+,(i+1)-}\right.$$
$$\left. - \Phi^{(3)}_{i-,i+,i+}\right](b'-b) + \Phi^{(3)}_{i+,i+,(i+1)-}(a'-a),$$

$$\text{(3a)}$$

$$\tilde{\Phi}^{(2)}_{i-,i+} = \Phi^{(2)}_{i-,i+} + \frac{1}{2}\left[\Phi^{(3)}_{(i-1)+,i-,i+} + \Phi^{(3)}_{i-,i+,i+}\right.$$
$$\left. - \Phi^{(3)}_{i-,i+,(i+1)-} - \Phi^{(3)}_{i-,i-,i+}\right](b'-b)$$
$$+ \left[\Phi^{(3)}_{i-,i+,(i+1)-} - \Phi^{(3)}_{(i-1)+,i-,i+}\right](a'-a),$$

$$\text{(3b)}$$

$$\tilde{\Phi}^{(2)}_{i+,(i+1)-} = \Phi^{(2)}_{i+,(i+1)-} + \frac{1}{2}\left[\Phi^{(3)}_{i+,i+,(i+1)-} + \Phi^{(3)}_{i+,(i+1)-,(i+1)+}\right.$$
$$\left. - \Phi^{(3)}_{i+,(i+1)-,(i+1)-} - \Phi^{(3)}_{i-,i+,(i+1)-}\right](b'-b)$$
$$+ \left[\Phi^{(3)}_{i+,(i+1)-,(i+1)-} + \Phi^{(3)}_{i+,(i+1)-,(i+1)+}\right]$$
$$\times (a'-a),$$

$$\text{(3c)}$$

$$\tilde{\Phi}^{(2)}_{i-,i-} = \Phi^{(2)}_{i-,i-} + \frac{1}{2}\left[-\Phi^{(3)}_{i-,i-,i-} + \Phi^{(3)}_{(i-1)+,i-,i-}\right.$$
$$\left. + \Phi^{(3)}_{i-,i-,i+}\right](b'-b) - \Phi^{(3)}_{(i-1)+,i-,i-}(a'-a).$$

$$\text{(3d)}$$

Considering only the nearest neighboring terms of the third-order derivatives, the force constant in Eq. (3) can be rewritten as

$$\tilde{\Phi}^{(2)}_{i-,i+} = -\beta_1 + \delta_1(b'-b),\qquad\text{(4a)}$$

$$\tilde{\Phi}^{(2)}_{i+,(i+1)-} = -\beta_2 - \delta_2(b'-b) + \delta_2(a'-a),\quad\text{(4b)}$$

$$\tilde{\Phi}^{(2)}_{i+,i+} = \tilde{\Phi}^{(2)}_{i-,i-} = \beta_1 + \beta_2 + (\delta_2-\delta_1)(b'-b)$$
$$- \delta_2(a'-a).\qquad\text{(4c)}$$

Here we denote $\Phi^{(2)}_{i+,i-} = -\beta_1$, $\Phi^{(2)}_{i+,(i+1)-} = -\beta_2$, $\Phi^{(2)}_{i+,i+} = \Phi^{(2)}_{i-,i-} = \beta_1 + \beta_2$, $\Phi^{(3)}_{i+,i+,i-} = -\Phi^{(3)}_{i+,i-,i-} = \delta_1$, $\Phi^{(3)}_{i+,i+,(i+1)-} = -\Phi^{(3)}_{i+,(i+1)-,(i+1)+} = -\delta_2$, $\Phi^{(3)}_{i+,i+,i+} = -\Phi^{(3)}_{i-,i-,i-} = -\delta_1 + \delta_2$. The relations $\sum_{i'v'}\Phi^{(2)}_{iv,i'v'} = 0$ and $\sum_{i'v',i''v''}\Phi^{(3)}_{iv,i'v',i''v''} = 0$ are used in the calculations.

The variation of force constants shown in Eq. (4) will change the sound velocity from $v_s = a\sqrt{\beta_1\beta_2/(\beta_1+\beta_2)(M_+ + M_-)}$ to

$$v'_s \approx v_s\frac{a'}{a}$$
$$\times\sqrt{1 - \frac{\beta_2^2\delta_1 - \beta_1^2\delta_2}{2\beta_1\beta_2(\beta_1+\beta_2)}(b'-b) - \frac{\beta_1\delta_2}{\beta_2(\beta_1+\beta_2)}(a'-a)},$$

$$\text{(5)}$$

with accuracy to the first order of the variation of $\Phi^{(2)}_{iv,i'v'}$. The variation of a and b induced by the electric field can be estimated from the piezoelectric effect and dielectric properties [25]:

$$\frac{a'-a}{a} = d_{33}E,\quad b'-b = -\left(\frac{\Omega}{\bar{M}}\right)^{\frac{1}{2}}\frac{b_{12}}{b_{11}}E,\qquad\text{(6)}$$

where d_{33} is the piezoelectric coefficient, $b_{11} = -\omega_0^2$, and $b_{12} = [\varepsilon(0) - \varepsilon(\infty)]^{1/2}\varepsilon_0^{1/2}\omega_0$. Ω is the volume per unit cell, $\bar{M} = M_+M_-/(M_+ + M_-)$ is the reduced mass, ω_0 is the frequency of the transverse optic mode, ε_0 is the permittivity of free space, $\varepsilon(0)$ is the static dielectric constant, and $\varepsilon(\infty)$ the high-frequency dielectric constant. It is obvious that both $a'-a$ and $b'-b$ are linearly dependent on E. One can easily find that $v'_s \approx v_s(1 + d_{33}E)\sqrt{1+\gamma E}$, where γ can be determined from Eq. (5). A simplified symmetric case of $\delta = (\delta_1/\beta_1^2) - (\delta_2/\beta_2^2) = 0$ leads to a limiting form of γ that shows that

$$\gamma_s = \lim_{\delta\to 0}\gamma = -\frac{v_s^2}{k_B}(M_- + M_+)\alpha_1 d_{33},\qquad\text{(7)}$$

where $\alpha_1 = \frac{k_B}{2a}\left(\frac{\delta_1}{\beta_1^2} + \frac{\delta_2}{\beta_2^2}\right)$ is the thermal expansion coefficient and k_B is the Boltzmann coefficient. If we ignore the changes in scattering strength and specific heat, the thermal conductivity of the polymer is proportional to its sound velocity [7]. Then the electric field dependence of thermal conductivity due to phonon renormalization is $\kappa \propto (1 + d_{33}E)\sqrt{1+\gamma E}$. We point out that γ should be of the same order as γ_s. The difference between them is attributed to the detailed molecular chain conformation in real polymer as illustrated in Fig. 1(d). The reason is that there are many other effects that have not been considered in our model: (1) bond angle variation; (2) chain orientation; (3) crystallinity; (4) phase transition of the polymer [there are two phases of P(VDF-TrFE)]; and (5) bond length variation [17,26]. We notice that $(v_s^2/k_B)(M_- + M_+)\alpha_1 \gg 1$ is usually satisfied in ferroelectric polymers, and then the thermal conductivity of ferroelectric polymer under electric field is

$$\kappa \approx \kappa_0\sqrt{1+\gamma E},\qquad\text{(8)}$$

where κ_0 is the thermal conductivity in the absence of an electric field.

III. EXPERIMENTAL DETAILS

We test our phonon renormalization theory by studying the electric field dependence of thermal conductivity of P(VDF-TrFE) nanofibers. For this material γ_s is estimated to be $3.5\,\mathrm{nm\,V^{-1}}$ by using $d_{33} = -55 \times 10^{-3}\,\mathrm{nm\,V^{-1}}$ [27], $\alpha_1 = 6.6 \times 10^{-4}\,\mathrm{K^{-1}}$ [27], $M_- + M_+ = 2.31 \times 10^{-25}\,\mathrm{kg}$ [28] and $v_s = 2400\,\mathrm{m\,s^{-1}}$ [29]. Conventional PVDF is mainly composed of nonpolar gauche isomers (α-phase), which leads to week ferroelectricity [30]. The ferroelectricity of P(VDF-TrFE) can be enhanced by introducing more β-phase from larger polymerization ratio of trifluoroethylene (TrFE). In this experiment, we prepare P(VDF-TrFE) nanofibers of 70/30 molar ratios and implemented definite posttreatments. Figure 2(a) shows X-ray diffraction spectra of P(VDF-TrFE) powders and electrospinning nanofibers. The presence of a dominant peak at $2\theta = 20°$, which corresponds to the β-phase [30], confirms that both powders and

(a)

(b)

FIG. 2. (a) X-ray diffraction results of P(VDF-TrFE) 70/30 powders and nanofibers. The marked β-phase is generally considered as the ferroelectric phase. (b) SEM image of the single P(VDF-TrFE) nanofiber suspended on the device for thermal conductivity measurement. The scale bar is 10 μm. Insert: the enlarged SEM image of the same P(VDF-TrFE) nanofiber. The scale bar is 500 nm.

nanofibers possess intrinsic ferroelectricity. Figure 2(b) shows that a suspended P(VDF-TrFE) nanofiber formed across the two suspended SiN_x membranes by electrospinning technology. After electrospinning, the suspended P(VDF-TrFE) nanofibers need to be annealed at 140 °C in N_2 to improve their crystallization [25]. The two SiN_x membranes are covered by platinum (Pt) coils, acting as heater and temperature sensor for thermal conductivity measurement. Two Pt/SiN_x electrodes at the middle of the whole microdevice are used to apply an electric field along the axis of the nanofibers. To avoid the interaction between a plurality of nanofibers, we chose a suspended single nanofiber; note, however, that it is extremely difficult for electrospinning to measure the polarization tunable thermal conductivity. In order to observe the change in thermal conductivity caused by the external field, the whole suspended microdevice is placed in a cryostat with high vacuum of the order of 1×10^{-5} Pa to reduce the thermal convection. Since the change of thermal conductivity of P(VDF-TrFE) nanofibers would be much lower than the measurement sensitivity of the traditional thermal bridge method [31,32], we adopt the differential circuit configuration in our experiments due to its advanced measurement sensitivity approaching to $10\,\mathrm{pW\,K^{-1}}$ [33,34].

Two samples are prepared such that the diameter and length of sample 1 (sample 2) are 138 nm (511 nm) and 1.95 μm (1 μm), respectively. The ferroelectricity of the polymer is sensitive to its postprocessing condition [35]. Therefore, we further treat sample 1 with three different postprocessing methods (referred to as samples 1a, 1b,
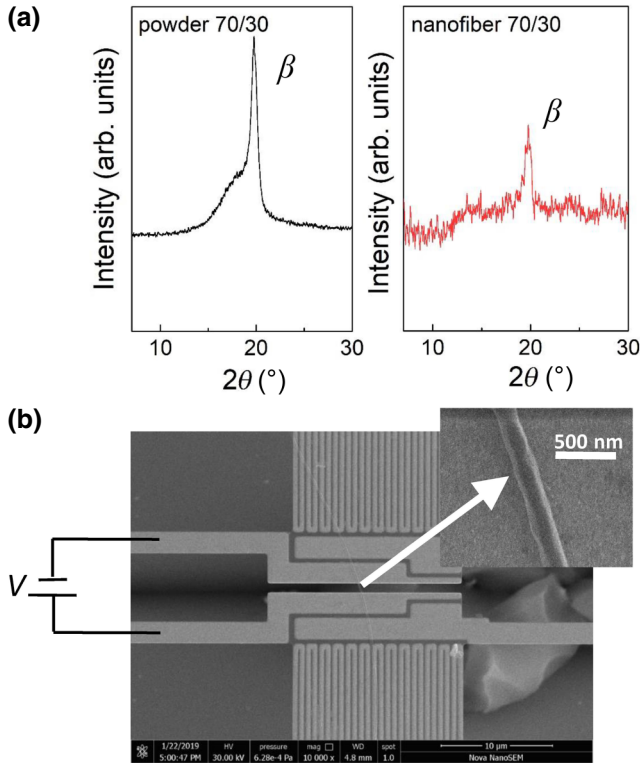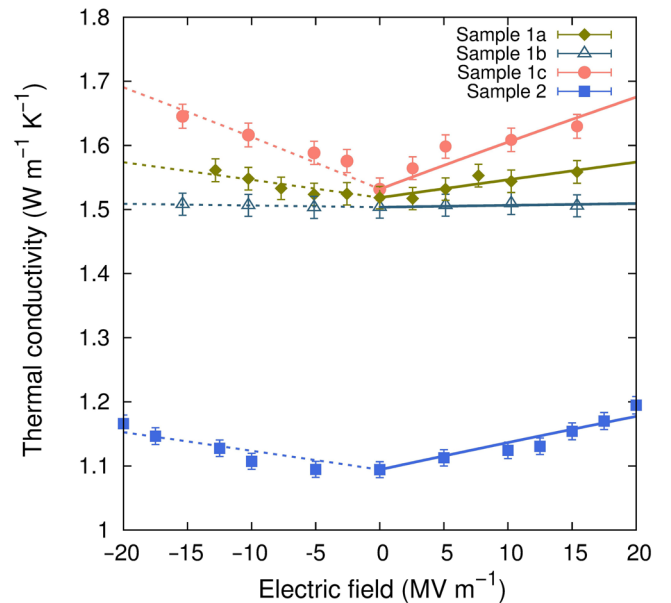

FIG. 3. Electric field dependence of the thermal conductivity at 300 K of samples under different annealing conditions. Solid dots are measured data and lines are fitted by Eq. (8).

TABLE I. The fitted γ and γ/γ_s of different P(VDF-TrFE) nanofibers.

Sample	Annealing condition	κ_0 (W m^{-1} K^{-1})	γ (nm V^{-1})		γ/γ_s	
			Positive field	Negative field	Positive field	Negative field
1a	140 °C; N$_2$; 30 min furnace cooling	1.52	3.7 ± 0.5	3.7 ± 0.4	1.1	1.1
1b	67 °C; vacuum; bake	1.50	0.4 ± 0.2	0.35 ± 0.07	—	—
1c	140 °C; N$_2$; 2 h slow cooling	1.53	9.8 ± 1.2	10.9 ± 1.0	2.8	3.1
2	140 °C; N$_2$; 30 min furnace cooling	1.10	7.9 ± 0.6	5.5 ± 0.7	2.3	1.5

and 1c) before each measurement. Sample 1a and sample 2 are annealed in nitrogen at 140 °C, followed by furnace cooling; sample 1b is baked in a high-vacuum cryostat at 67 °C; sample 1c is annealed in nitrogen at 140 °C, followed by a slow cooling (2 h), which is a recrystallization process.

IV. RESULTS AND DISCUSSION

The measured thermal conductivity of all the samples under positive and negative electric fields at $T = 300$ K is shown in Fig. 3. It is shown that thermal conductivity increases with the electric field. The electric field dependence of measured thermal conductivity of samples 1a, 1c, and 2 are in good agreement with Eq. (8). The fitted values of γ are listed in Table I. For sample 1a, γ equals 1.1 γ_s for both positive and negative fields. The fitted γ of sample 1c, which is cooled slowly after annealing, is 2.8γ_s for positive field and 3.1 γ_s for negative field. The larger γ corresponding to sample 1c originates from a larger fraction of β-phases after the recrystallizing process, which gives rise to a higher piezoelectricity. As for sample 2 with larger diameter, γ is 2.3γ_s for positive field and 1.5γ_s for negative field. There are two possible reasons for the slight difference between different field directions: (1) when changing the direction of voltage, the remnant polarizability partially compensates the electric field poling effect; (2) when $\delta_1/\beta_1^2 \neq \delta_2/\beta_2^2$, γ changes when the electric field changes direction according to Eq. (5). It is interesting to note that the thermal conductivity of sample 1b does not change with the electric field. This result is consistent with the morphology of the sample; it has been reported that P(VDF-TrFE) transforms from trans conformers (β-phase) to gauche isomers (α-phase) around 60 °C in a vacuum, and consequently the ferroelectricity will be largely reduced [36]. Macroscopically, sample 1b has an ignorable piezoelectric effect, thus γ is too small to observe. From the above results, we find that the ferroelectricity is essential to achieve the phonon renormalization. Large crystallinity of ferroelectric phase and better chain orientation are preferred.

V. CONCLUSION

In summary, we reveal that the electric field could induce phonon renormalization in ferroelectric polymers.

The measured thermal conductivity of ferroelectric P(VDF-TrFE) nanofibers exhibits a monotonic increasing behavior under an electric field, which is in good agreement with our analytical phonon renormalization model. The tunable molecular chain structure under an electric field and reversible phase transition are a promising prospect in the future application of polymer ferroelectrics.

[1] T. Tadano and S. Tsuneyuki, Quartic Anharmonicity of Rattlers and its Effect on Lattice Thermal Conductivity of Clathrates From First Principles, Phys. Rev. Lett. **120**, 105901 (2018).

[2] D. B. Zhang, T. Sun, and R. M. Wentzcovitch, Phonon Quasiparticles and Anharmonic Free Energy in Complex Systems, Phys. Rev. Lett. **112**, 058501 (2014).

[3] N. B. Li, J. J. Liu, C. Q. Wu, and B. Li, Temperature and frequency dependent mean free paths of renormalized phonons in nonlinear lattices, New J. Phys. **20**, 023006 (2018).

[4] J. J. Liu, S. Liu, N. B. Li, B. Li, and C. Q. Wu, Renormalized phonons in nonlinear lattices: A variational approach, Phys. Rev. E **91**, 042910 (2015).

[5] M. M. Koza, M. R. Johnson, R. Viennois, H. Mutka, L. Girard, and D. Ravot, Breakdown of phonon glass paradigm in La-and Ce-filled Fe 4 Sb 12 skutterudites, Nat. Mater. **7**, 805 (2008).

[6] R. Picu, T. Borca-Tasciuc, and M. Pavel, Strain and size effects on heat transport in nanostructures, J. Appl. Phys. **93**, 3535 (2003).

[7] W. P. Hsieh, M. D. Losego, P. V. Braun, S. Shenogin, P. Keblinski, and D. G. Cahill, Testing the minimum thermal conductivity model for amorphous polymers using high pressure, Phys. Rev. B **83**, 174205 (2011).

[8] X. Li, K. Maute, M. L. Dunn, and R. Yang, Strain effects on the thermal conductivity of nanostructures, Phys. Rev. B **81**, 245318 (2010).

[9] N. Wei, L. Xu, H. Q. Wang, and J. C. Zheng, Strain engineering of thermal conductivity in graphene sheets and nanoribbons: A demonstration of magic flexibility, Nanotechnology **22**, 105705 (2011).

[10] F. Ma, H. Zheng, Y. Sun, D. Yang, K. Xu, and P. K. Chu, Strain effect on lattice vibration, heat capacity, and thermal conductivity of graphene, Appl. Phys. Lett. **101,** 111904 (2012).

[11] L. F. C. Pereira and D. Donadio, Divergence of the thermal conductivity in uniaxially strained graphene, Phys. Rev. B **87,** 125424 (2013).

[12] S. Bhowmick and V. B. Shenoy, Effect of strain on the thermal conductivity of solids, J. Chem. Phys. **125,** 164513 (2006).

[13] K. F. Murphy, B. Piccione, M. B. Zanjani, J. R. Lukes, and D. S. Gianola, Strain-and defect-mediated thermal conductivity in silicon nanowires, Nano Lett. **14,** 3785 (2014).

[14] L. Zhu and X. Zheng, Modification of the phonon thermal conductivity in spatially confined semiconductor nanofilms under stress fields, Europhys. Lett. **88,** 36003 (2009).

[15] X. Huang, G. Liu, and X. Wang, New secrets of spider silk: Exceptionally high thermal conductivity and its abnormal change under stretching, Adv. Mater. **24,** 1482 (2012).

[16] G. Qin, Z. Qin, S. Y. Yue, Q. B. Yan, and M. Hu, External electric field driving the ultra-low thermal conductivity of silicene, Nanoscale **9,** 7227 (2017).

[17] V. S. Bystrov, E. V. Paramonova, I. K. Bdikin, A. V. Bystrova, R. C. Pullar, and A. L. Kholkin, Molecular modeling of the piezoelectric effect in the ferroelectric polymer poly(vinylidene fluoride) (PVDF), J. Mol. Model. **19,** 3591 (2013).

[18] C. Liu, Y. Chen, and C. Dames, Electric-Field-Controlled Thermal Switch in Ferroelectric Materials Using First-Principles Calculations and Domain-Wall Engineering, Phys. Rev. Appl. **11,** 044002 (2019).

[19] J. F. Ihlefeld, B. M. Foley, D. A. Scrymgeour, J. R. Michael, B. B. McKenzie, D. L. Medlin, M. Wallace, S. Trolier-McKinstry, and P. E. Hopkins, Room-temperature voltage tunable phonon thermal conductivity via reconfigurable interfaces in ferroelectric thin films, Nano Lett. **15,** 1791 (2015).

[20] S. Ning, S. C. Huberman, C. Zhang, Z. Zhang, G. Chen, and C. A. Ross, Dependence of the Thermal Conductivity of BiFeO3 Thin Films on Polarization and Structure, Phys. Rev. Appl. **8,** 054049 (2017).

[21] P. E. Hopkins, C. Adamo, L. Ye, B. D. Huey, S. R. Lee, D. G. Schlom, and J. F. Ihlefeld, Effects of coherent ferroelastic domain walls on the thermal conductivity and Kapitza conductance in bismuth ferrite, Appl. Phys. Lett. **102,** 121903 (2013).

[22] P. Guin and A. Roy, Design of efficient loadcell for measurement of mechanical impact by piezoelectric PVDF film sensor, AIP Adv. **6,** 095122 (2016).

[23] M. M. Abolhasani, F. Zarejousheghani, Z. Cheng, and M. Naebe, A facile method to enhance ferroelectric properties in PVDF nanocomposites, RSC Adv. **5,** 22471 (2015).

[24] M. Owczarek, K. A. Hujsak, D. P. Ferris, A. Prokofjevs, I. Majerz, P. Szklarz, H. Zhang, A. A. Sarjeant, C. L. Stern, and R. Jakubas, Flexible ferroelectric organic crystals, Nat. Commun. **7,** 13108 (2016).

[25] K. Huang, On the interaction between the radiation field and ionic crystals, Proc. R. Soc. London A **208,** 352 (1951).

[26] V. V. Kochervinskiĭ, Structural changes in ferroelectric polymers under the action of strong electric fields by the example of polyvinylidene fluoride, Crystallogr. Rep. **51,** S88 (2006).

[27] A. Aliane, M. Benwadih, B. Bouthinon, R. Coppard, D. D. Santos, and A. Daami, Impact of crystallization on ferro-, piezo- and pyro-electric characteristics in thin film P(VDF–TrFE), Org. Electron. **25,** 92 (2015).

[28] F. C. Sun, A. M. Dongare, A. D. Asandei, P. Alpay, and S. Nakhmanson, Temperature dependent structural, elastic, and polar properties of ferroelectric polyvinylidene fluoride (PVDF) and trifluoroethylene (TrFE) copolymers, J. Mater. Chem. C **3,** 8389 (2015).

[29] K. Koga and H. Ohigashi, Piezoelectricity and related properties of vinylidene fluoride and trifluoroethylene copolymers, J. Appl. Phys. **59,** 2142 (1986).

[30] G. Ren, F. Cai, B. Li, J. Zheng, and C. Xu, Flexible pressure sensor based on a poly(VDF-TrFE) nanofiber web, Macromol. Mater. Eng. **298,** 541 (2013).

[31] P. Kim, L. Shi, A. Majumdar, and P. L. McEuen, Thermal Transport Measurements of Individual Multiwalled Nanotubes, Phys. Rev. Lett. **87,** 215502 (2001).

[32] X. Xu, L. F. Pereira, Y. Wang, J. Wu, K. Zhang, X. Zhao, S. Bae, C. T. Bui, R. Xie, and J. T. Thong, Length-dependent thermal conductivity in suspended single-layer graphene, Nat. Commun. **5,** 3689 (2014).

[33] L. Dong, Q. Xi, D. Chen, J. Guo, T. Nakayama, Y. Li, Z. Liang, J. Zhou, X. Xu, and B. Li, Dimensional crossover of heat conduction in amorphous polyimide nanofibers, Natl. Sci. Rev. **5,** 500 (2018).

[34] M. C. Wingert, Z. C. Chen, S. Kwon, J. Xiang, and R. Chen, Ultra-sensitive thermal conductance measurement of one-dimensional nanostructures enhanced by differential bridge, Rev. Sci. Instrum. **83,** 024901 (2012).

[35] M. Baniasadi, X. Zhe, S. Moreno, S. S. Daryadel, J. Cai, M. Naraghi, and M. Minary-Jolandan, Effect of thermomechanical post-processing on chain orientation and crystallinity of electrospun P(VDF-TrFE) nanofibers, Polymer **118,** 223 (2017).

[36] G. Teyssedre and C. Lacabanne, Study of the thermal and dielectric behavior of P(VDF-TrFE) copolymers in relation with their electroactive properties, Ferroelectrics **171,** 125 (1995).